GEOCHRONOMETRIA 48 (2021): 222–231
DOI 10.2478/geochr-2020-0011

Available online at
https://content.sciendo.com/view/journals/geochr/geochr-overview.xml

Conference Proceedings of the 5th Asia Pacific Luminescence and Electron Spin Resonance Dating Conference October 15th-17th, 2018, Beijing, China

Guest Editor: Grzegorz Adamiec

COMPONENT-RESOLVED ANALYSIS TOWARDS CORRELATION BETWEEN THERMOLUMINESCENCE AND OPTICALLY STIMULATED LUMINESCENCE IN COMMERCIAL MAGNESIUM OXIDE

NIYAZI MERIÇ[1], EREN ŞAHINER[1], GEORGE KITIS[2] and GEORGE S. POLYMERIS[1]
[1]*Institute of Nuclear Sciences, Ankara University, Beşevler, 06100-Ankara, Turkey*
[2]*Aristotle University of Thessaloniki, Nuclear Physics Laboratory, 54124-Thessaloniki, Greece*

Received 15 January 2019 Accepted 31 October 2019

Abstract: The present study aimed at quantifying the relationship between TL and either CW-OSL or LM-OSL using commercially available magnesium oxide. The samples were bleached at two different temperatures, and a component-resolved analysis on the integrated signals was performed. According to the data of the present study, each one among the five observed LM-OSL component receives electrons from at least two different TL peaks. Two different fast OSL components were resolved in the LM-OSL curves, both accumulating electrons from all TL glow peaks with T_{max}>150°C. Component C_3 is very well correlated with the TL peaks at 102, 135 and 194°C, while components C_4 and C_5 are related to the TL glow peaks of 292°C, 353°C and 464°C. We note that for CW-OSL the resolution is good when two or more components differ in intensity by an order of magnitude. Blue stimulation depletes substantially the first two TL peaks but not the third peak. Substantial depletion of the high-temperature TL peaks is achieved only by using the LM-OSL configuration. The results of the present study suggest that the traps that contribute to TL and OSL are the same, despite using different recombination pathways.

Keywords: MgO, OSL, TL, component resolved analysis, Lambert W function.

1. INTRODUCTION

Luminescence in all forms, namely thermoluminescence (TL), infrared stimulated luminescence (IRSL) and optically stimulated luminescence (OSL), arises from band to band transitions and impurity ions or intrinsic defects. These impurities inside the matrix of the luminescence materials give rise to localised energy levels within the forbidden energy band gap. Luminescence dosimetry nowadays represents a key technique in absorbed dose measurements (Furetta, 2003). While IRSL and OSL are mostly used for dosimetry/dating purposes, TL is an experimental technique used in diverse scientific disciplines, which, besides dosimetry, include archaeology, geology, medical and solid state physics. It is well known that every geological inorganic material, insulator or semiconductor, which has been previously exposed to ionising radiation, could be a potential luminescent dosimeter in action; in other words, it could yield lumines-

Corresponding author: N. Meriç
e-mail: meric@ankara.edu.tr

ISSN 1897-1695 (online), 1733-8387 (print)

cence signal. The process in which absorbed energy is converted into luminescence light can be distinguished in different steps, each one characterised by certain efficiency. Materials with high total efficiency are characterised as sensitive TL dosimeters (TLDs) (Bos, 2001).

Nowadays, the term oxidation refers to all processes involving the loss of electrons. Nevertheless, originally the word oxidation implied a chemical reaction with oxygen to form an oxide since the gas O_2 was historically the first recognised oxidising agent. For many areas of materials science, a reaction in the presence of O_2, and thus subsequent degradation, stands as one of the primary instability mechanisms. For instance, in practical thermoelectric applications, apart from high efficiency, excellent thermal stability at the intended operating temperature range is of vital importance (Yin *et al.,* 2015). Thus, degradation of high-temperature Mg_2Si thermoelectric devices through oxidation is one of the primary examples in the field of thermoelectrics, as in the presence of O_2, Mg_2Si decomposes to form MgO and Si (Tani *et al.,* 2009). Nevertheless, while for the field of thermoelectrics, the presence of oxides is not welcome for the operational stability, in the field of TL dosimetry, a variety of oxides have been effectively applied as sensitive TLDs. Aluminium oxide (Al_2O_3:C) (Akselrod and Kortov, 1990; Markey *et al.,* 1995) and beryllium oxide (BeO) (Sommer and Henniger, 2006; Sommer *et al.,* 2007, 2008; Yukihara, 2019a, 2019b; Aşlar *et al.*, 2019) stand among the most distinguished members of this list; for an extended review on the oxides used as TLDs, the readers could refer to McKeever *et al.* (1995).

Magnesium oxide (MgO), in its un-doped form, also yields sufficient TL sensitivity. Its potential applicability in TL dosimetry was exploited many decades ago (Roessler and Walker, 1967; Ziniker *et al.,* 1973; Takeuchi *et al.,* 1976; Carter, 1976). Nevertheless, due to a number of reasons, which include (a) composite glow curve structure, (b) relatively low sensitivity and (c) high variability of its TL properties depending on the synthesis technique, magnesium oxide has not found wide acceptance as a practical TL detector. Some of the earlier results have been reviewed by McKeever *et al.* (1995). Many researchers aimed towards optimisation of its luminescence properties, by adopting different synthesis methodologies as well as doping (Bapat and Sivaraman, 1985; Bapat *et al.,* 1985; Dolgov *et al.,* 2002; Bos *et al.,* 2006; Oliveira *et al.,* 2013). According to a recent report, using a combination of the Solution Combustion Synthesis (SCS) method, doping with different lanthanides (Ln) and co-doping with lithium (Li) can considerably increase the sensitivity of MgO (Orante-Barron *et al.,* 2011). Nevertheless, according to this latter citation, the lanthanide doping was reported to affect not only the luminescence centres but also the shape of the TL curve. An extensive review of the defects in MgO and their relationship with its TL properties can be found in Las and Stoebe (1984).

The present work attempts a correlation between TL and OSL signals observed in MgO phosphor via a bleaching study. By the term bleaching, we refer to the effect of the eviction of a significant proportion of the trapped electrons abandoning thus the traps when the dosimeter is exposed to artificial or natural light. The physical mechanisms that govern the effect of bleaching are yet to be thoroughly understood. Moreover, even though the bleaching properties of TL traps in various materials seem to be a both unmapped as well as very important topic of research from a physical point of view, very few related works have been reported so far in the literature. Among these, special emphasis should be addressed to those reported by Spooner (1994) and Kitis *et al.* (2010) for the case of quartz and Dallas *et al.* (2010) for the case of $KMgF_3:Ce^{3+}$. Very recently, Sfampa *et al.* (2015), Kitis *et al.* (2016) as well as Angeli *et al.* (2019) have individually attempted correlation of basic TL, OSL and IRSL properties of various K-feldspar samples and other geological samples. According to those mentioned above, scanty reports of related literature, all luminescence forms make use of the same traps, namely TL traps. Further establishing this latter experimental statement/feature becomes the primary aim of the present study.

2. EXPERIMENTAL PROCEDURE

Sample, apparatus and measurement conditions

The study was performed on natural magnesium oxide sample, *MgO*. This specific sample was selected mainly for two reasons: (a) the convenient shape of its glow curve, consisting of two, prominent and independent groups of overlapping peaks and (b) the lack of any previous related studies on this specific material. The commercial *MgO* sample was purchased from Sigma Aldrich. Grains of dimensions between 80 μm and 140 μm were obtained after dry sieving. Aliquots with the mass of 5 mg each were prepared by mounting the material on stainless-steel disks of 1 cm^2 area. Mass reproducibility was kept within ±5%.

All luminescence measurements were carried out using a Risø TL/OSL Reader (model TL/OSL–DA–20), equipped with a high power blue LED light source (470 nm, FWHM 20 nm delivering at the sample position a maximum power of 40 mW/cm^2) and a $^{90}Sr/^{90}Y$ beta particle source, delivering a nominal dose rate of 0.1083 Gy/s (Bøtter-Jensen *et al.,* 2000). A 9635QB photomultiplier tube with a Hoya (U-340) blue filter was used for light detection (340 nm, FWHM 80nm). All TL measurements and heatings were performed in a nitrogen atmosphere with a low constant heating rate of 1°C/s, in order to avoid significant temperature lag (Kitis *et al.,* 2015); TL measurements were performed up to the maximum temperature of 500°C. OSL measurements were performed in both continuous wave as well as linearly

modulated configurations (CW-OSL and LM-OSL, respectively). In the former case, the power level was software controlled and set at 90% of the maximum stimulation intensity for blue LEDs. For LM-OSL curves (Bulur, 1996), the ramping rate was 0.04 mW/cm^2/s, increasing the stimulation light power from zero up to the maximum power (40 mW/cm^2) for 1000 s.

Experimental Protocols

Bleaching can take place in nature either spontaneously or under strict experimental conditions. In the latter case, measuring the number of optically de-trapped electrons that are emitted following stimulation, results in optically stimulated luminescence (OSL) curves. In the framework of the present study, bleaching was performed by exposing the samples to the blue LEDs housed inside the Risø commercial TL/OSL Reader, stimulating at 90% of their maximum stimulation intensity (40 mW/cm^2, Bøtter-Jensen *et al.,* 2000). Similar bleaching studies were also performed in the past for the case of quartz (Polymeris *et al.,* 2012). The experimental procedure involved two basic protocols. The first one (protocol A) was applied in order to investigate the bleaching of the entire glow curve; therefore the OSL measurements were performed at room temperature (RT hereafter), according to the following protocol that consists of the following steps:

Step 0: Test Dose and TL measurement for the un-bleached signal in order to monitor the un-bleached signal.

Step 1: Test Dose and CW-OSL measurement for stimulation time t_i=1 s.

Step 2: TL measurement in order to obtain the residual TL.

Step 3: Steps 1&2 were repeated using different stimulation times t_i= 2, 4, 8, 16, 32, 64, 128, 256, 512, 1024 and 2048 s.

The second protocol (protocol B) was applied in order to investigate the bleaching of the high temperature part of the glow curve. In this case, the protocol mentioned above was applied, after incorporating the following two modifications; (a) before each OSL measurement, a TL up to 180°C was performed, in order to empty all shallow traps and (b) the OSL measurements were performed at 170°C in order to prevent re-trapping of charge evicted from the deeper traps into shallow peaks.

The test dose applied was 20 Gy. According to the related literature, *MgO* does not yield sensitivity changes following successive cycles of irradiation and TL measurements. Therefore, each one of the protocols described above was applied to two independent aliquots, implying thus a single aliquot procedure. Nevertheless, performing sensitivity variation tests was inevitable. Three sensitivity tests were performed by recording a TL glow-curve for a test dose of 20 Gy, one after the RTL corresponding to 8 s bleaching, one after the RTL corresponding to 128 s bleaching and one, final, after the final step of 2048 s bleaching. The resulted TL glow-curves showed a reproducibility within 2%, which means that there is no need for sensitivity corrections. Finally, after the application of each protocol characteristic LM-OSL curves were obtained for a stimulation time of 1000 s.

3. METHOD OF ANALYSIS

The entirely empirical general order kinetics can be considered as an approach to the elementary OTOR model (Sadek *et al.,* 2014a, 2014b). Recently, Kitis and Vlachos (2012) showed that the OTOR system of differential equations can be solved analytically using the Lambert W(z) function. The analytical expression derived by them is advantageous, because it is a general equation describing all commonly used luminescence stimulation modes. In other words, the same equations can describe TL, linearly modulated OSL (LM-OSL), continuous wave optically stimulated luminescence (CW-OSL), Isothermal TL (ITL) and others, by just setting the corresponding stimulation mode.

The original equation derived by Kitis and Vlachos (2012) as a solution of the OTOR model is the following:

$$I(T) = \frac{N \cdot R}{(1-R)^2} \cdot \frac{p(t,T)}{W(z)+W(z)^2} \tag{3.1}$$

where N is the total concentration of trapping states and $W(z)$ is the Lambert W function (Corless *et al.,* 1996), and $R=A_n/A_m$ with A_n, A_m being the re-trapping and recombination coefficients correspondingly. In the present work **Eq. 3.1** will be used considering only the case $R < 1$ (Corless *et al.,* 1996; Kitis and Vlachos, 2012, Sadek *et al.,* 2014a). The function $p(t, T)$ in **Eq. 3.1** deals with the stimulation mode used during the experiments. For the case of TL is $p(T) = s \cdot exp(-E/kT)$ so, the argument z of the Lambert function $W(z)$ becomes:

$$z = \exp\left(\frac{R}{1-R} - \ln\left(\frac{1-R}{R}\right) \cdot \frac{s}{\beta \cdot (1-R)} \int_{T_0}^{T} e^{-\frac{E}{kT}} dT\right) \tag{3.2}$$

For the case of LM-OSL, $p(T) = \lambda t$ so, the argument z of the Lambert function $W(z)$ becomes:

$$z = \exp\left(\frac{R}{1-R} - \ln\left(\frac{1-R}{R}\right) + \frac{\lambda t^2}{2 \cdot (1-R)}\right) \tag{3.3}$$

For the case of exponential decay, $p(T) = \lambda$ so, the argument z of the Lambert function $W(z)$ becomes:

$$z = \exp\left(\frac{R}{1-R} - \ln\left(\frac{1-R}{R}\right) + \frac{\lambda t}{(1-R)}\right) \tag{3.4}$$

In the case of TL the original **Eq. 3.1** was transformed by Sadek *et al.,* (2014b), so that the parameters N and s were replaced by the maximum TL intensity of the peak I_m and by the temperature of the peak maximum T_m. This is a very useful substitution, since these two quantities I_m and T_m can be obtained directly and accurately from the experimental TL glow curves.

The final equation (given by Sadek *et al.,* 2014b) is the following:

$$I(T) = I_m exp\left(-\frac{E}{kT}\cdot\frac{T_m-T}{T_m}\right)\cdot\frac{W(z_m)+W(z_m)^2}{W(z)+W(z)^2} \quad (3.5)$$

where z is now approximated by the expression:

$$z = \exp\left(\frac{R}{1-R} - \ln\left(\frac{1-R}{R}\right) + \frac{E\cdot\exp(\frac{E}{kT_m})}{kT_m^2(1-1.05\cdot R^{1.26})}\cdot F(T,E)\right) \quad (3.6)$$

and z_m is the value of z for $T = T_m$ according to **Eq. 3.6**.

Eqs. 3.5 and **3.6** are the analytical equations used to fit the experimental TL glow curves, with the two adjustable fitting parameters being the activation energy E and the ratio R (with $R < 1$).

The function $F(T,E)$ in this expression is the exponential integral appearing in TL models and is expressed in terms of the exponential integral function $Ei[-E/kT]$ as (Chen and McKeever, 1997; Kitis *et al.*, 2006):

$$F(T,E) = \int_{T_0}^{T} e^{-\frac{E}{kT}}dT = T\cdot exp\left(-\frac{E}{kT}\right) + \frac{E}{k}\cdot E_i\left[-\frac{E}{kT}\right] \quad (3.7)$$

For the LM-OSL we have:

$$I(T) = I_m\cdot\frac{t}{t_m}\cdot\frac{W(z_m)+W(z_m)^2}{W(z)+W(z)^2} \quad (3.8)$$

where z is now approximated by the expression:

$$z = \exp\left(\frac{R}{1-R} - \ln\left(\frac{1-R}{R}\right) + \frac{t^2}{t_m^2}\cdot\frac{1.0455-0.3869\cdot R^{0.4647}}{2\cdot(1-R)}\right) \quad (3.9)$$

and z_m is the value of z for $t = t_m$ according to **Eq. 3.9**.

The application of the Lambert function $W(z)$ is quite complicated when one has to use analytical approximations for it (Kitis and Vlachos, 2012). On the other hand, its application is very simple in commercial software packages (for example MATHEMATICA, MATLAB) which include it as a built-in function, similar to any other transcendental function. In the present work, the ROOT data Analysis Framework was used (ROOT, 2015). All fittings were performed using the MINUIT program (MINUIT, 2015) released in ROOT, which is a physics-analysis tool for function minimisation. The Lambert function $W(z)$ and the exponential integral function $Ei[-E/kT]$ are implemented in ROOT through the GNU scientific library (GNU GSL) (GNU, 2015). The goodness of fit was tested using the Figure Of Merit (FOM) of Balian and Eddy (1977) given by:

$$FOM(\%) = 100 * \sum_p |TL_{exp} - TL_{fit}| / \sum_p TL_{fit} \quad (3.10)$$

The FOM index value provides a measure for the goodness of fit; the lowest its value, the best fit we get. Therefore, every fitting attempt should result in minimising the FOM index value, which was achieved by changing the set of parameter values of each glow peak.

4. RESULTS AND DISCUSSION

Experimental luminescence curve shapes

As it is seen from the experimental protocol, the bleaching of the TL glow-curve of MgO is achieved through CW-OSL stimulation. All these CW-OSL curves were recorded; typical shapes of these are shown in **Fig. 1**. The latter figure contains the normalised CW-OSL curves corresponding to stimulation times of 128, 256, 512, 1024 and 2048 s, which coincide. This experimental fact is a direct evidence of the excellent reproducibility of the measuring sequence. The most interesting detail of these curves is the very fast decay in short stimulation times. The same results are also observed for the rest of the CW-OSL curves obtained.

The shapes of residual TL (R-TL) glow-curves as a function of the bleaching time from 1 to 2048 s are shown in **Fig. 2**. The TL glow-curve has a characteristic low temperature glow-peak and a number of overlapped high temperature glow-peaks. Similar are the shapes for the case of the OSL curves after preheat at 170°C, without yielding the shallow peak at around 100°C. According to the data of this latter plot, it is possible to conclude that

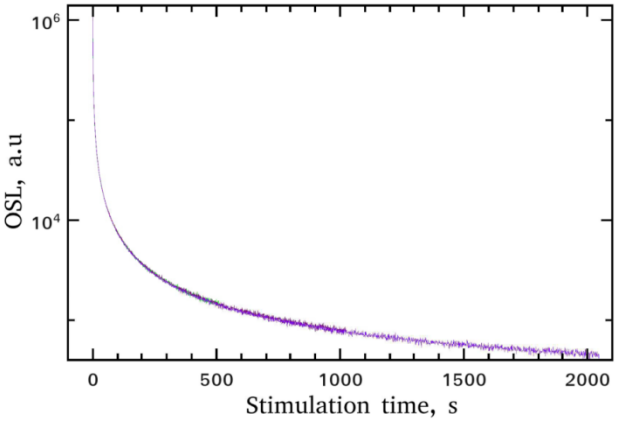

Fig. 1. *CW-OSL decay curves received at room temperature, using blue light for stimulation times 128, 256, 512, 1024 and 2048 s, which coincide. This experimental feature yields the excellent reproducibility the measuring sequence.*

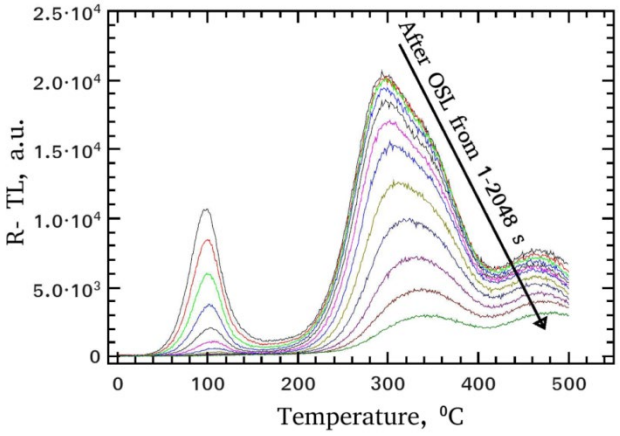

Fig. 2. *Shapes of the R-TL glow-curves received after bleaching with blue light for all stimulation times, ranging between 1 and 2048 s.*

the shallow trap responsible for the low temperature TL peak is easily and fast bleached within stimulation time intervals between 2 s and 20 s. On the contrary, the overlapping peaks located at higher temperatures survive for small stimulation times. Nevertheless, for stimulation durations longer than 100 s, this complex TL peak is also substantially bleached.

Studying a tentative correlation between the individual TL peaks and OSL components requires the complete analysis of the complex TL glow-curves, which will be presented in detail in section 4 – Analysis of TL glow-curves. **Fig. 3** shows the shape of the LM-OSL curves corresponding to each one of the two protocols. The basic characteristic is the very intense fast component obtained in very short stimulation times, exactly as in the case of CW-OSL shown in **Fig. 1**.

A very interesting result is the quantitative relationship between the integrated signals of the TL-glow-curves and the CW-OSL curves depicted in **Fig. 4**. The relationship is expressed in terms of the ratio between the integrated OSL signal over the integrated TL-lost signal, where TL-lost is the difference between the un-bleached glow-curve minus the bleached glow-curve at each bleaching (OSL stimulation) time. This difference corresponds to the number of electrons which are getting free due to optical bleaching, which recombining gives the CW-OSL intensity. Therefore, from a phenomenological point of view, it is expected that the ratio will always take values around unity. This theoretical expectation is not verified by the experiment mainly at very short OSL stimulation durations.

As it is seen in **Fig. 4**, the integrated CW-OSL signal is much higher than the corresponding TL-lost in both stimulation temperatures for stimulation times less than 20 s. As the stimulation time increases, the ratio tends to unity, in agreement with the theoretical predictions. The direct conclusion concerning the first 20 s of stimulation is that the very high intensity CW-OSL signal corresponds to negligible variation of R-TL curves in the region of the high temperature glow-curve (200–500°C). This observation is crucial for the subsequent analysis of the data and for the final conclusions on the TL and OSL correlation in next sections.

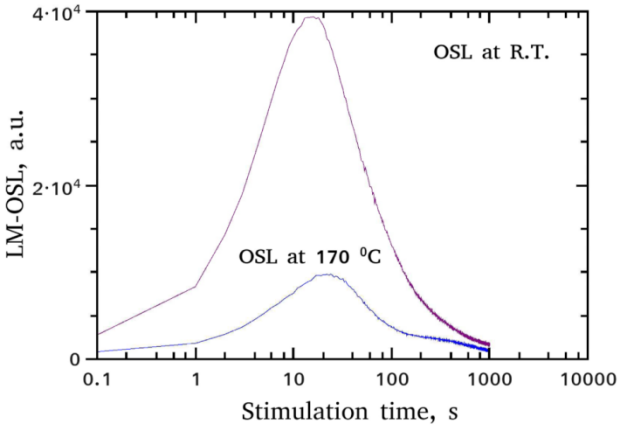

Fig. 3. *Shapes of the LM-OSL curves received at RT and at 170°C after a pre-heat at 180°C.*

Analysis of TL glow-curves

Twelve (12) R-TL glow-curves were obtained in the framework of protocol 1; these are presented in **Fig. 2** along with the corresponding twelve (12) glow-curves obtained in the framework of the protocol 2. Both sets of R-TL curves were analysed using a computerised glow-curve de-convolution (CGCD) using **Eq. 3.5** with z according to **Eq. 3.6**. Furthermore, the CGCD analysis was also performed using the equations for conventional general order kinetics by Kitis *et al.* (1998). The FOM values obtained were below 1% up to bleaching (stimulation) time of 256 s and between 1 and 2% for bleaching times 512, 1024 and 2048 s. The higher FOM values for the latter cases could be explained by the fact that, due to prolonged bleaching, the intensity of the TL glow curve becomes of poorer statistics. The values of the trapping parameters obtained throughout the fitting analysis are shown in **Table 1**. The fit of the glow-curves of both protocols was performed with a remarkable stability of the free parameters E and T_m. Furthermore, an excellent agreement between the results of OTOR analytical TL equation and general order kinetics equation was achieved. The errors of E and T_m represent errors of the mean value between the results of the two equations used. Their meaning is twofold, providing besides the error values also the degree of agreement between OTOR analytical equation and general order equation. The agreement achieved was necessary because the general order is

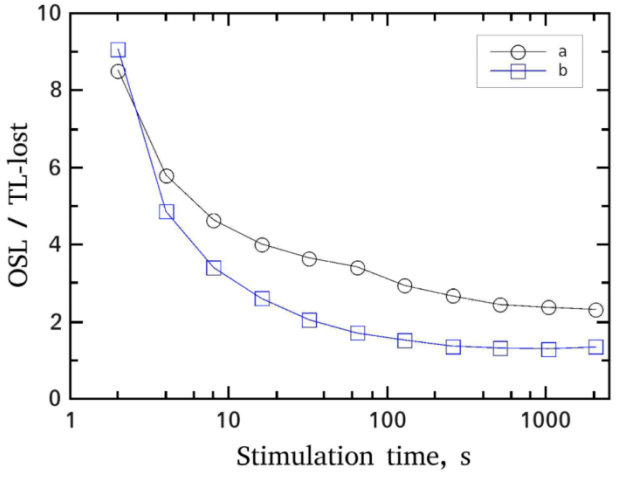

Fig. 4. *The ratio of integrated CW-OSL over the TL-lost during the various stimulation times. The TL-lost is defined as the difference between the total integrals of the un-bleached glow-curve minus the bleached TL glow-curves (a) For OSL measured at RT and (b) for OSL measured at 170°C.*

Table 1. *The values of the trapping parameters of MgO resulting from the CGCD analysis using both general order kinetics and OTOR analytical equation.*

Peak no.	T_m (°C)	E (eV)	R	b	%OSL (RT)	%OSL (170°C)
1	102 ± 2	0.90 ± 0.09	0.42 ± 0.07	1.40 ± 0.02	12.50	-
2	132 ± 1	0.94 ± 0.11	0.76 ± 0.17	1.97 ± 0.05	1.50	-
3	194 ± 2	0.82 ± 0.03	0.90 ± 0.06	1.55 ± 0.05	1.55	1.30
4	292 ± 4	1.13 ± 0.05	0.65 ± 0.16	1.60 ± 0.10	38.12	50.44
5	353 ± 3	1.24 ± 0.03	0.81 ± 0.04	1.90 ± 0.07	30.64	32.94
6	464 ± 2	1.45 ± 0.04	0.71 ± 0.07	1.79 ± 0.17	15.27	14.59

an empirical approach of the OTOR analytical equation; as it was shown in detail by Sadek *et al.* (2014a, 2014b) for R < 1 their differences are negligible. Furthermore, **Table 1** shows the values of re-trapping to recombination probability ratio, *R*, the kinetic order *b* and finally the percentages of the individual TL peaks for un-bleached glow-curves without and with pre-heat at 180°C.

Fig. 5 presents the results of CGCD analysis of the glow-curves from protocol 1. The experimental points (presented as open circles) and the fitted line are given only for the R-TL after 1 s OSL bleaching. The glow-peaks with continuous lines correspond to the CGCD results of all other R-TL glow-curves shown in **Fig. 2**. The two very low intensity glow-peaks 2 and 3 at 134 and 194°C respectively, are not included in the figure. The integrated signal of each of the peaks in **Fig. 5**, as well as the sum of the peaks 2 and 3, will be used for the forthcoming analysis in next section.

Analysis of R-TL decay curves

The plot of R-TL signal versus bleaching time has the form of decay curve. Since the decay of R-TL is caused by the optical bleaching, despite its thermal stimulation origin, it reflects the optical bleaching dynamics. For this reason, the analysis of R-TL versus bleaching time will be performed with analytical expressions describing OSL decay curves such as **Eq. 3.1** with z from **Eq. 3.4**. Furthermore, the RTL decay analysis was also performed using the conventional general order kinetics equation (Bulur, 1996). Since, as it was stated above, the R-TL decay behaviour reflects the bleaching dynamics, it is expected that the lifetimes of **Table 2** should be related to the lifetimes yielded using the general order kinetics equation by Bulur (1996). It must be noticed, however, that Bulur's equation for CW-OSL is, typologically, identical with the general order kinetics equation describing the decay of TL at a constant temperature. Similarly, **Eq. 3.1** with z from **Eq. 3.4** also describes the TL decay at a constant temperature. The difference is that in OSL the decay constant represents the optical photoionisation cross-section and in TL decay thermal escape probability.

As it is shown in **Fig. 5**, the CGCD analysis gives the individual TL peaks of the glow-curve. The integrated signal of each peak is plotted as a function of the bleaching time and then fitted using **Eq. 3.1** with z from **Eq. 3.4** and equation from Bulur (1996). It was not possible to fit the R-TL versus bleaching time using one component, so two components C_1 and C_2 were used, making thus the analysis very sensitive. Fitting examples are given in **Fig. 6**. The fitting parameters are listed in **Table 2**. As is the case of TL CGCD results listed in **Table 1** (section 4 – Analysis of TL glow-curves) the values of the lifetime

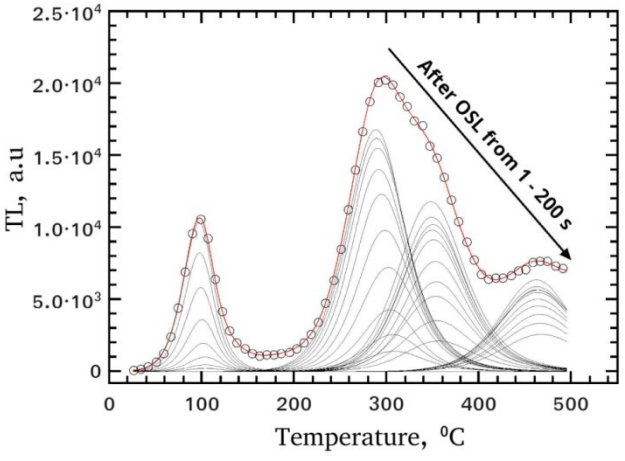

Fig. 5. *Results of the CGCD analysis of RTL glow-curves after CW-OSL at RT using Eqs. 3.5 and 3.6. The open circles represent the experimental glow-curve after CW-OSL for 1 s. The line through the experimental points is the fitting line. The continuous lines present the results of the CGCD of all R-TL glow-curves of Fig. 2 without the repeating of the experimental curves. The results for fitting parameters are listed in Table 1.*

Table 2. *The fitting parameters of the RTL integrated signals as a function of the bleaching time using both general order and OTOR analytical equations. The values are the mean between of the values obtained by the two different equations. The error values provide a strong indication towards the agreement of the two different Equations used.*

Peak T_m (°C)	OSL T	τ_1 (s)	%	τ_2 (s)	%
102	RT	6.34 ± 0.71	90	75 ± 11	10
134+194	RT	5.68 ± 1.91	85	150 ± 40	15
292	RT	276 ± 15	72	2726 ± 380	28
353	RT	130 ± 31	28	2350 ± 280	72
464	RT	221 ± 25	20	2750 ± 360	80
292	170°C	98 ± 7	58	782 ± 42	42
353	170°C	85 ± 18	20	828 ± 40	80
464	170°C	55 ± 10	07	1920 ±210	93

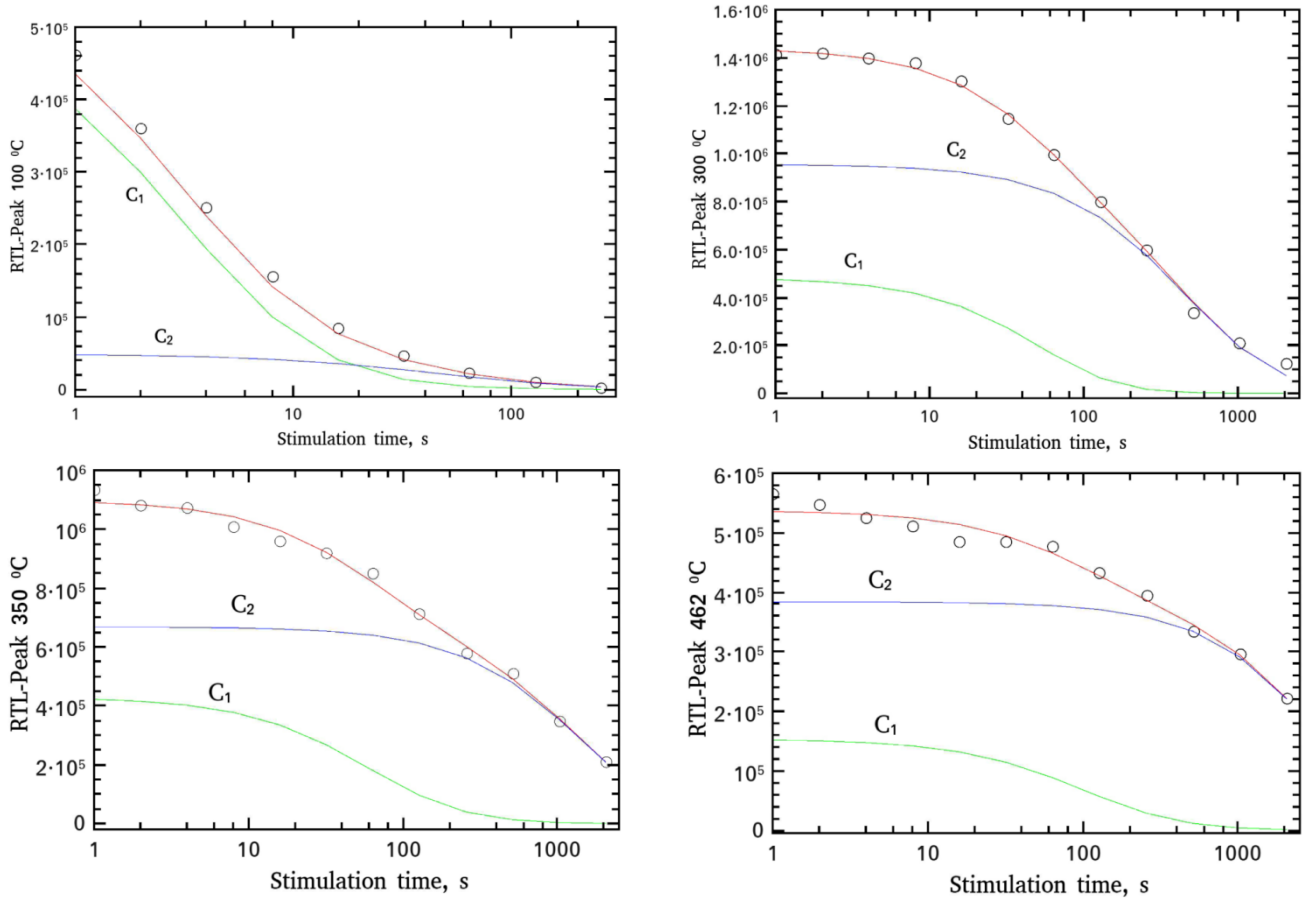

Fig. 6. *Analysis examples of R-TL decay curves based on the integrated signal of the main R-TL glow-peaks resulted from CGCD analysis shown individually in Fig.5. The fit was performed using Eqs. 3.1 and 3.4. The results of the fitting parameters are listed in Table 2.*

correspond to the mean between the results of OTOR analytical expression and general order kinetics. The error value is again a measure of the agreement between the OTOR decay equation and general order kinetics decay equation.

Since the R-TL decay behaviour reflects the bleaching dynamics, it is expected that the lifetimes of **Table 2** should be related to the lifetimes from an analysis of an LM-OSL curve. In the present work, LM-OSL curves were obtained for a simulation time of 1000 s. Their analysis is presented in the next section.

Analysis of the LM-OSL curves

Both LM-OSL curves received at RT and at 170°C, were analysed through a CGCD procedure using **Eq. 3.8** and z according to **Eq. 3.9**. Alternatively, as in the CGCD of TL, the general order kinetics equation of Bulur (1996) as it was modified by Kitis and Pagonis (2008), was used. The analysed LM-OSL curves are shown in **Fig. 7**, whereas the fitting parameter values are listed in **Table 3**. Additionally, the percentage of each component for the two LM-OSL curves are presented below. The free parameter t_m in column 2 was transformed into a lifetime in column 3 using the conditions for the maximum which as it was shown by Kitis and Vlachos (2012), providing thus identical results for both OTOR analytical equation and Bulur's (1996) general order kinetics equation. The values of the parameter t_m and of the per component percentage, as in the previous cases, is the mean between OTOR and general order kinetics equations, whereas its error is a measure of their agreement.

TL and OSL correlation

A tentative correlation will be based on the comparison of the results of **Tables 2** and **3**. Obviously, a correlation cannot be achieved just by setting the requirement of exactly equal lifetimes (τ values), because (a) the physical meaning of the lifetime τ is not exactly similar in R-TL and LM-OSL and (b) the values of LM-OSL strongly depend on the total LM-OSL stimulation time. On the other hand, the values must not differ appreciably because both R-TL and LM-OSL take place in the same time interval. A correlation will be attempted by trying to detect the values of LM-OSL curves (**Table 3**) in the values of R-TL decay curves (**Table 2**).

Table 3. *The fitting parameters from the analysis of the LM-OSL curve using both general order and OTOR analytical equations. The values are the mean between of the values obtained by the two different equations. Error values provide a strong indication towards the agreement of the two different Equations used.*

Component	OSL T	t_m (s)	τ (s)	R	b	%
C_1	RT	5.38 ± 0.45	0.036 ± 0.003	0.6	1.7	2 ± 0.15
C_2	RT	15.64 ± 0.22	0.306 ± 0.003	0.7	1.8	23.3 ± 1.1
C_3	RT	55.9 ± 4.1	3.9 ± 0.003	0.83	1.9	35.5 ± 4
C_4	RT	248 ± 38	76.9 ± 0.003	0.93	1.8	31.9 ± 2.9
C_5	RT	1151 ± 450	1667 ± 0.003	0.01	1.1	7.29 ± 0.16
C_1	170°C	4.33 ± 0.7	0.024 ± 0.003	0.68	1.6	0.74 ± 0.18
C_2	170°C	20.01 ± 0.40	0.506 ± 0.003	0.83	1.65	17.5 ± 1.3
C_3	170°C	53 ± 0.5	3.51 ± 0.003	0.81	1.8	16.4 ± 0.5
C_4	170°C	244.8 ± 9.5	74.42 ± 0.003	0.94	1.9	43.9 ± 2.1
C_5	170°C	723 ± 92	653 ± 0.003	0.51	1.4	21.4 ± 2.5

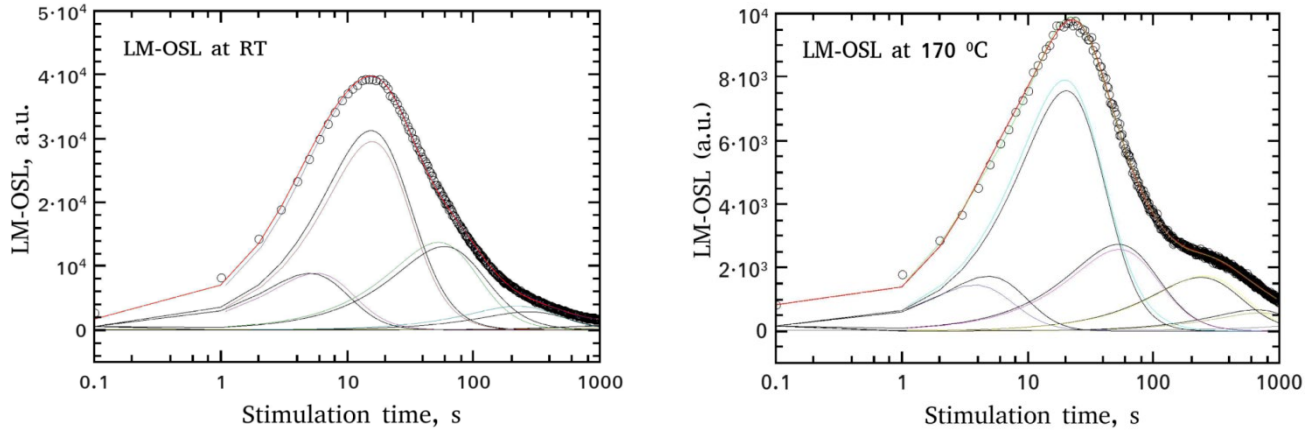

Fig. 7. *Component resolved of LM-OSL curves received at RT and at 170°C after a pre-heat at 180°C, using Eqs. 3.8 and 3.9. The results of the fitting parameters are listed in Table 3.*

Components C_1 and C_2

The origin of the very fast components C_1 and C_2 of the LM-OSL curves shown in **Fig. 7** become of great interest; the corresponding fitting parameters are listed in **Table 3**. In the case of LM-OSL measured at RT, these components appear in the LM-OSL curves, because the stimulation power starts from very low value. On the contrary, in the case of CW-OSL the stimulation power takes its highest value immediately. The result is that in CW-OSL curves, these components contribute only to the first second of stimulation, so they cannot be resolved. On the other hand during the two seconds of CW-OSL stimulation when these components have been exhausted due their short lifetime, only the TL intensity of the R-TL for the TL peak at 102°C is reduced, whereas the higher temperature TL peaks have been not influenced at all.

A correlation of these components with the 102°C TL peak is not possible, because these components also appear in LM-OSL curves received at 170°C after a pre-heat up to 180°C, which erases this latter TL peak completely. Finally, as it can be easily seen in **Table 3**, these components with the percentage of 25% of the total LM-OSL signal are related to a negligible TL-lost. So, the net conclusion is that resolution of the correlation method used in the present work is not capable of detecting any relation between the energy levels responsible for the TL peaks and the energy levels responsible for the components C_1 and C_2 of the LM-OSL signal.

Component C_3

Component C_3 is very well correlated with the TL peaks at 102, 135 and 194°C. These peaks contribute almost 16% of the TL signal and 25.2% of the LM-OSL signal received at RT. However, although these peaks are erased by the pre-heat at 180°C, component C_3 appears also at LM-OSL received at 170°C, representing the 18% of the corresponding signal. Therefore, component C_3 originates not only from the peaks with delocalisation temperatures of 102°C, 135°C and 194°C. On the other hand the analysis of R-TL from high temperature peaks does not yield its presence in the region of the high temperature TL glow-peaks. The reason lies behind the reso-

lution of the method. Indeed, component C_3 having a lifetime of 4 s is decayed up to OSL stimulation time of less than 20 s. However, as it is seen in **Fig. 2**, the decreases of the R-TL signal from 1 to 16 s is very weak, so this component cannot be resolved accurately by the method used.

In the case of LM-OSL curve obtained at RT, the components C_1, C_2 and C_3 correspond to the 60% of the total LM-OSL signal. Subtracting the 15% which corresponds to the TL peaks of 102°C, 135°C and 194°C, then a percentage of 45% of the LM-OSL signal cannot be directly correlated, by the method used, with any other TL peak. In the case of LM-OSL recorded at 170°C, components C_1, C_2 and C_3 correspond approximately the 35% of the total LM-OSL signal. Taking into account that the peaks 102°C, 135°C and 194°C are erased by the pre-heat at 170°C then the entire percentage of 35% of these components cannot be related, by the method used, to any of the TL peaks.

Component C_4

Another question deals with whether the values of lifetimes τ_1 of the peaks at 292°C, 353°C and 464°C could be reflected to the component C_4. In order to answer to this question, a discussion about the resolution of the LM-OSL curves is necessary. In a detailed resolution study, Kitis and Pagonis (2008) showed that two overlapping LM-OSL peaks can be resolved if their time at peak maximum intensity, t_m, differs by more than 15%. Based on this resolution value and as it is seen in **Table 2**, the lifetimes of the corresponding to the R-TL decay of peaks at 292 and 464°C are quite close to each other. Taking also into account that the contribution of the TL peak at 292°C is much higher, then it can be easily concluded that their discrimination in LM-OSL curve is very difficult. On the other hand, corresponding to the TL peak at 353°C is quite different but with relatively low contributions. So, the conclusion concerning the LM-OSL curve received at RT cannot be more than a quantitative relationship of LM-OSL component C_4 with the first component of the R-TL decay curves.

Concerning the LM-OSL curves received at 170°C after a pre-heat to 180°C, the lifetime values τ_1 are very close to the lifetime value of LM-OSL component C_4. So, in this case it is quite safe to correlate the first component of the R-TL decay curves of TL peaks at 292°C, 353°C and 464°C, with the component C_4 of the LM-OSL curve.

Component C_5

In the previous sections, a correlation based only on the first component of the R-TL decay curves was discussed. The reason is that the lifetime of the second R-TL component is equal and mainly greater than the LM-OSL stimulation time. This means that these components should correspond to LM-OSL peaks having peak maximum (t_m) at times beyond the 1000 s. The consequence is that in LM-OSL only the rise part of such high t_m LM-OSL peaks is recorded without any possibility of separation. Therefore, any LM-OSL signal correlated with the 2 of **Table 2** will be degenerated in one only component. In the present case this is the LM-OSL component C_5, which obviously is complex and originates from the second component of the R-TL decay curves of peaks at 292°C, 353°C and 464°C.

5. CONCLUSIONS

A component resolved bleaching analysis was conducted to the luminescence signal of commercial magnesium oxide. Bleaching took place at two different temperatures, namely at RT without any preheat as well as at 170°C after a preheat at 180°C, towards a quantitative relationship between the integrated signals of the TL-glow-curves and either the CW-OSL or LM-OSL curves. According to the data of the present study:

1) The integrated CW-OSL signal is much higher than the corresponding lost TL signal for both stimulation temperatures for stimulation times less than 20 s. However, as the stimulation time is increased, OSL and TL lost signal are of similar magnitude.
2) The analytical solution of the OTOR system of differential equations using the Lambert function W(z) provides de-convolution results with great accuracy for all cases of TL, CW-OSL and LM-OSL curves.
3) The fast OSL components C_1 and C_2 were monitored as consisting of electrons originated from all TL peaks. Therefore, these two components could not be correlated to any individual TL glow peak.
4) Component C_3 is very well correlated with the TL peaks at 102, 135 and 194°C, while components C_4 and C_5 are directly correlated to the TL glow peaks of 292°C, 353°C and 464°C.
5) The dosimetric properties of components C_4 and C_5 should be further exploited.

REFERENCES

Akselrod MS and Kortov VS, 1990. Thermoluminescent and exoemission properties of new high-sensitivity TLD α-Al2O3:C crystals. *Radiation Protection Dosimetry* 33(1–4): 123–126.

Angeli V, Kitis G, Polymeris GS, Şahiner E and Meriç N, 2019. Component-resolved bleaching correlation between OSL and IRSL signals in various geological materials. *Applied Radiation and Isotopes* 143: 156–162, DOI 10.1016/j.apradiso.2018.10.018.

Aşlar E, Meriç N, Şahiner E, Erdem O, Kitis G and Polymeris GS, 2019. A correlation study on the TL, OSL and ESR signals in commercial BeO dosimeters yielding intense transfer effects. *Journal of Luminescence* 214: 116533, DOI 10.1016/j.jlumin.2019.116533.

Balian HG and Eddy NW, 1977. Figure Of Merit (FOM): an improved criterion over the normalised chi-square test for assign the goodness-of-fit of gamma ray spectral peaks. *Nuclear Instruments and Methods* 145: 389–395.

Bapat MN and Sivaraman S, 1985. The role of Ce^{3+} in the luminescence of MgO. *Indian Journal of Pure and Applied Physics*: 23: 535–536.

Bapat MN, Sivaraman S and Nambi DSV, 1985. Thermoluminescence of MgO:Li(Ce, Eu). *Indian Journal of Pure and Applied Physics* 23: 558–560.

Bos AJJ, 2001. High sensitivity thermoluminescence dosimetry. *Nuclear Instruments and Methods in Physics Research B* 184: 3–28, DOI 10.1016/S0168-583X(01)00717-0.

Bos AJJ, Prokić M and Brouwer JC, 2006. Optically and thermally stimulated luminescence characteristics of MgO:Tb^{3+}. *Radiation Protection Dosimetry* 119: 130–133, DOI 10.1093/rpd/nci641.

Bøtter-Jensen L, Bulur E, Duller GAT and Murray AS, 2000. Advances in luminescence instrument systems. *Radiation Measurements* 32: 523–528, DOI 10.1016/S1350-4487(00)00039-1.

Bulur E, 1996. An alternative technique for optically stimulated luminescence (OSL) experiment. *Radiation Measurements* 26: 701–704, DOI 10.1016/S1350-4487(97)82884-3.

Carter AC, 1976. Thermoluminescence of magnesium oxide. *Nature* 260: 133–134, DOI 10.1038/260133a0.

Chen R and McKeever SWS, 1997. *Theory of Thermoluminescence and Related Phenomena*, World Scientific.

Corless RM, Gonnet GH, Hare DGE, Jeffrey DJ and Knuth DE, 1996. On the Lambert W function. *Advances in Computational Mathematics* 5: 329–359, DOI 10.1007/BF02124750.

Dallas GI, Polymeris GS, Afouxenidis D, Tsirliganis NC, Tsagas NF and Kitis G, 2010. Correlation between TL and OSL signals in $KMgF_3:Ce^{3+}$: Bleaching study of individual glow-peaks. *Radiation Measurements* 45: 537–539, DOI 10.1016/j.radmeas.2009.11.008.

Dolgov S, Kärner T, Luschik A, Maaroos A, Mironova-Ulmane N and Nakonechnyi S, 2002. Thermoluminescence Centres Created Selectively in MgO Crystals by Fast Neutrons. *Radiation Protection Dosimetry*, 100: 127–130, DOI 10.1093/oxfordjournals.rpd.a005828.

Furetta C, 2003. *Handbook of Thermoluminescence*. World Scientific, Singapore.

GSL-GNU Scientific Library, 2015. www.gnu.org/software/gsl.

Kitis G, Chen R, Pagonis V, Carinou E and Kamenopoulou V, 2006. Thermoluminescence under an exponential heating function: I. Theory. *Journal of Physics D-Applied Physics* 39: 1500–1507, DOI 10.1088/0022-3727/39/8/008.

Kitis G, Kiyak N, Polymeris GS and Tsirliganis NC, 2010. The correlation of fast OSL component with the TL peak at 325°C in quartz of various origins. *Journal of Luminescence* 130: 298–303, DOI 10.1016/j.jlumin.2009.09.006.

Kitis G, Kiyak NG and Polymeris GS, 2015. Temperature lags of luminescence measurements in a commercial luminescence reader. *Nuclear Instruments and Methods in Physics Research Section B* 359: 60–63, DOI 10.1016/j.nimb.2015.07.041.

Kitis G and Pagonis V, 2008. Computerized curve deconvolution analysis for LM – OSL. *Radiation Measurements* 43: 737–741, DOI 10.1016/j.radmeas.2007.12.055.

Kitis G, Polymeris GS, Şahiner E, Meriç N and Pagonis V, 2016. Influence of the infrared stimulation on the optically stimulated luminescence in four K-feldspar samples. *Journal of Luminescence* 176: 32–39, DOI 10.1016/j.jlumin.2016.02.023.

Kitis G and Vlachos ND, 2012. General semi-analytical expressions for TL, OSL and other luminescence stimulation modes derived from the OTOR model using the Lambert W-function. *Radiation Measurements* 48: 47–54, DOI 10.1016/j.radmeas.2012.09.006.

Kitis G, Gomez Ros JM and Tuyn JWN, 1998. Thermoluminescence glow-curve deconvolution function for first, second and general order kinetics. *Journal of Physics D-Applied Physics* 31: 2065–2073, DOI 10.1088/0022-3727/31/19/037.

Las WC and Stoebe TG, 1984. TL Mechanisms and Luminescence Characteristics in MgO. *Radiation Protection Dosimetry* 8: 45–67.

Markey BG, Colyott LE and McKeever SWS, 1995. Time-resolved optically stimulated luminescence from α-Al_2O_3:C. *Radiation Measurements* 24: 457–463, DOI 10.1016/1350-4487(94)00119-L.

McKeever SWS, Moscovitch M and Townsend PD, 1995. *Thermoluminescence Dosimetry Materials: Properties and Uses.* Nuclear Technology Publishing.

MINUIT, a Physics Analysis Tool for Function Minimization. Released in ROOT, 2015.

Oliveira LC, Doull BA and Yukihara EG, 2013. Investigations of MgO:Li,Gd thermally and optically stimulated luminescence. *Journal of Luminescence* 137: 282–289, DOI 10.1016/j.jlumin.2013.01.018.

Orante-Barron VR, Oliveira LC, Kelly JB, Milliken ED, Denis G, Jacobsohn LG, Puckette J and Yukihara EG, 2011. Luminescence properties of MgO produced by solution combustion synthesis and doped with lanthanides and Li. *Journal of Luminescence* 131: 1058–1065, DOI 10.1016/j.jlumin.2011.01.022.

Polymeris GS, Erginal AE and Kiyak NG, 2012. A comparative morphological, compositional and TL study of Tenedos (Bozcaada) and Şile aeolianites, Turkey. *Mediterranean Archaeology and Archaeometry* 12(2): 117–131.

Roessler DM and Walker WC, 1967. Electronic Spectrum and Ultraviolet Optical Properties of Crystalline MgO. *Physical Review* 159: 733, DOI 10.1103/PhysRev.159.733.

ROOT, A Data Analysis Framework, 2015. https://root.cern.ch.

Sadek AM, Eissa HM, Basha AM and Kitis G, 2014a. Resolving the limitation of the peak fitting and peak shape methods in the determination of the activation energy of thermoluminescence glow peaks. *Journal of Luminescence* 146: 418–423, DOI 10.1016/j.jlumin.2013.10.031.

Sadek AM, Eissa HM, Basha AM and Kitis G, 2014b. Development of the peak fitting and peak shape methods to analyse the thermoluminescence glow-curves generated with exponential heating function. *Nuclear Instruments and Methods in Physics Research Section B* 330: 103–107, DOI 10.1016/j.nimb.2014.04.006.

Sfampa IK, Polymeris GS, Pagonis V, Theodosoglou E, Tsirliganis NC and Kitis G, 2015. Correlation of basic TL, OSL and IRSL properties of ten K-feldspar samples of various origins. *Nuclear Instruments and Methods in Physics Research B* 359: 89–98, DOI 10.1016/j.nimb.2015.07.106.

Sommer M, Freudenberg R and Henniger J, 2007. New aspects of a BeO-based optically stimulated luminescence dosimeter. *Radiation Measurements* 42: 617–620, DOI 10.1016/j.radmeas.2007.01.052.

Sommer M and Henniger J, 2006. Investigation of a BeO-based optically stimulation luminescence dosimeter. *Radiation Protection Dosimetry* 119: 394–397, DOI 10.1093/rpd/nci626.

Sommer M, Jahn A and Henniger J, 2008. Beryllium oxide as optically stimulated luminescence dosimeter. *Radiation Measurements* 43: 353–356, DOI 10.1016/j.radmeas.2007.11.018.

Spooner NA, 1994. On the optical dating signal from quartz. *Radiation Measurements* 23: 593–600, DOI: 10.1016/1350-4487(94)90105-8.

Takeuchi N, Inabe K, Yamashita J and Nakamura S, 1976. Thermoluminescence of MgO single crystals for UV dosimetry. *Health Physics* 31: 519–521.

Tani JI, Takahashi MH and Kido H, 2009. Fabrication of oxidation-resistant β-$FeSi_2$ film on Mg_2Si by RF magnetron-sputtering deposition. Journal of Alloys and Compounds 488(1): 346–349, DOI 10.1016/j.jallcom.2009.08.128.

Yin K, Zhang Q, Zheng Y, Su X, Tang X and Uher C, 2015. Thermal stability of $Mg_2Si_{0.3}Sn_{0.7}$ under different heat treatment conditions. *Journal of Materials Chemistry C* 40: 10381–10387, DOI 10.1039/c5tc01434d.

Yukihara EG, 2019a. Observation of strong thermally transferred optically stimulated luminescence (TT-OSL) in BeO. *Radiation Measurements* 121: 103–108, DOI 10.1016/j.radmeas.2018.12.014.

Yukihara EG, 2019b. Characterisation of the thermally transferred optically stimulated luminescence (TT-OSL) of BeO. *Radiation Measurements* 126: 106132, DOI 10.1016/j.radmeas.2019.106132.

Ziniker WM, Rusin JM, Stoebe TG, 1973. Thermoluminescence and Activation Energies in Al2O3 and MgO and LiF(TLD-100). *Journal Of Materials Science* 8 407–413, DOI 10.1007/BF00550162.